

Self-Assembled Monolayers of Alkoxy-Substituted Octadehydrodibenzo[12]annulenes on a Graphite Surface: Attempts at *peri*-Benzopolyacene Formation by On-Surface Polymerization

Kazukuni Tahara,^[a] Koji Inukai,^[a] Noritaka Hara,^[a] Charles A. Johnson II,^[b] Michael M. Haley,^[b] and Yoshito Tobe^{*[a]}

Abstract: Self-assembled monolayers of a series of tetraalkoxy-substituted octadehydrodibenzo[12]annulene (DBA) derivatives **1c–g** possessing butadiyne linkages were studied at the 1,2,4-trichlorobenzene (TCB) or 1-phenyloctane/graphite interface by scanning tunneling microscopy (STM). The purpose of this research is not only to investigate the structural variation of two-dimensional (2D) monolayers, but also to assess a possibility for *peri*-benzopolyacene formation by two-dimensionally controlled polymerization on a surface. As a result, the formation of three structures, porous, linear, and lamella structures, were observed by changing the alkyl chain length and the

solute concentration. The formation of multilayers of the lamella structure was often observed for all compounds. The selection of molecular networks is basically ascribed to intermolecular and molecule–substrate interactions per unit area and network density. The selective appearance of the linear structure of **1d** is attributed to favorable epitaxial registry matching between the substrate lattice and the overlayer lattice. Even though the closest inter-

atomic distance between the diacetylenic units of the DBAs in the lamella structure (≈ 0.6 nm) is slightly larger compared to the typical distances necessary for topochemical polymerization, the reactivity toward external stimuli (electronic-pulse irradiation from an STM tip and UV irradiation) was investigated. Unfortunately, no evidence for polymerization of the DBAs on the surface was observed. The present results indicate the necessity for further designing a suitable system for the on-surface construction of structurally novel conjugated polymers, which are otherwise difficult to prepare.

Keywords: dehydrobenzoannulene • interfaces • monolayers • scanning probe microscopy • self-assembly

Introduction

Creation of two-dimensional (2D) architectures on solid surfaces based on molecular self-assembly has received great attention because of the prospective applications in the fields of nanoscience and nanotechnology,^[1,2] particularly in view of possible surface patterning in the low nanometer

regime.^[3] From the crystal engineering concept,^[4] to design and control of the structure and functionality, 2D molecular networks require investigations of the correlations between structural features of constituent molecules and the resulting topologies of surface-confined molecular architectures.^[5] In this respect, various types of 2D molecular networks have been investigated both under ultra-high vacuum (UHV) conditions and at liquid/solid interfaces.^[1,5]

In principle, to control 2D molecular networks, the following noncovalent interactions and experimental parameters must be taken into account. First, optimization of directional intermolecular interactions, which determine the network topology, such as hydrogen bonding,^[6] dipolar coupling,^[7] metal–ligand coordination,^[8] and van der Waals interactions between (sometimes interdigitating) alkyl chains^[9,10] is necessary. Molecule–substrate interactions (typically van der Waals interactions), which can be modulated by functional groups on molecules and choice of substrate,

[a] Dr. K. Tahara, K. Inukai, N. Hara, Prof. Dr. Y. Tobe
Division of Frontier Materials Science
Graduate School of Engineering Science
Osaka University, Toyonaka, Osaka 560-8531 (Japan)
Fax: (+81) 6-6850-6227
E-mail: tobe@chem.es.osaka-u.ac.jp

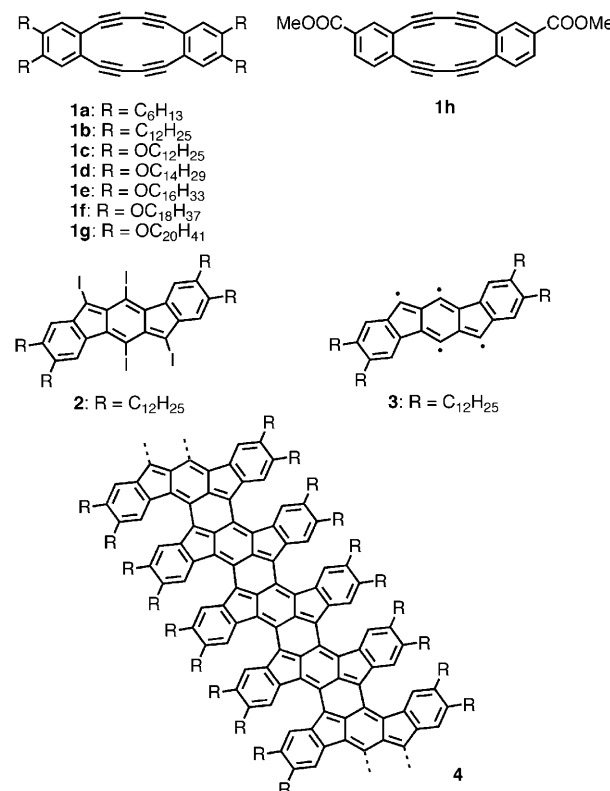
[b] Dr. C. A. Johnson II, Prof. Dr. M. M. Haley
Department of Chemistry and Materials Science Institute
University of Oregon, Eugene, OR 97403-1253 (USA)

 Supporting information for this article is available on the WWW under <http://dx.doi.org/10.1002/chem.201000711>.

are also important for the selection of network structures. In particular, epitaxial matching between the substrate and overlayer lattices would stabilize specific overlayer structures.^[11] At liquid/solid interfaces, solvents apparently play roles in network formation.^[12] For instance, solvents are often involved in the network (co-adsorption)^[13] and they affect the adsorption–desorption process too.^[14] Finally, various experimental conditions, such as timing of measurements,^[15] temperature,^[16] and solute concentration,^[17] are also known to influence the network formation. Scanning tunneling microscopy (STM) is a powerful tool to investigate 2D molecular networks with molecular scale precision and is typically used for this purpose.

Recently, special interest has been focused on covalently linked 2D molecular networks on surfaces, aiming at not only fixation of fragile 2D molecular networks, formed through noncovalent interactions, to construct robust 2D polymers,^[18] but also the formation of molecularly well-defined conducting polymers.^[19–21] Additionally, surface-specific reactions in a confined space would allow for the production of unique polymers otherwise unavailable by means of solution-phase reactions. The programmed reactions of molecular building blocks on solid surfaces, to generate the desired covalently linked 2D architectures, require precise molecular design. Pioneering works in this field were undertaken for topochemical 1,4-polymerization of diacetylene derivatives. For example, the first oligomerization of 17,19-hexatriacontadiyne on graphite by using UV irradiation has been investigated by means of UHV conditions.^[19] At a liquid/solid interface, De Schryver, De Feyter et al. reported that a monolayer of a diacetylene-containing isophthalic acid derivative underwent topochemical 1,4-polymerization upon UV irradiation to form a π -conjugated oligomer.^[20a,e] Subsequently, Aono et al. demonstrated nanoscale control of polymerization of 1,4-butadiyne derivatives on a surface by irradiation of an electronic pulse from an STM tip.^[20b,c] In these cases, strict control of spatial arrangement between the diacetylene units is necessary to initiate the topochemical 1,4-polymerization. Other types of covalent bond forming reactions on surfaces have been developed recently, such as imine formation between amines and aldehydes,^[22] ester formation between boronic acids and alcohols,^[23] and thermal and catalytic aryl–aryl coupling reactions.^[21,24] In some of these reactions, specific 2D spatial arrangement of the precursor molecules is required to achieve covalently-linked 2D architectures.

Among the various molecular building blocks, we chose octadehydronbenzo[12]annulene derivatives (DBAs, **1c–g**, Scheme 1)^[25] that possess two strained 1,3-butadiyne units, as potential precursors of π -conjugated polymers. DBA derivative **1a** was previously shown by Swager et al. to undergo oligomerization upon heating in the solid state, forming structurally undefined oligomers.^[26] Komatsu, Nishinaga et al. succeeded in controlling crystal structures of related DBA derivatives by utilizing stacking interactions of benzene and heavily fluorinated benzene moieties, but no well-defined polymers were obtained.^[27] Recently, Miyata, Hisaki



Scheme 1. Chemical structures of DBAs **1a–h**, tetriiododibenzoidiacene derivative **2**, hypothetical tetraradical intermediate **3**, and plausible *peri*-benzopolyacene **4** formed by lateral topochemical polymerization of the DBAs.

et al. reported gel formation of DBA derivative **1h**, but no topochemically controlled polymerization was attempted.^[28] In the stacked geometry of DBAs in crystals, the butadiyne units in a DBA molecule are expected to polymerize individually to form poly(butadiyne) moieties in the resultant tubular polymers.^[29] Contrary to polymerization, Swager et al. also reported the formation of tetriiododibenzoidiacene derivative **2** upon treatment of **1b** with iodine through transannular bond formation. Though the mechanism of this reaction is not certain, one may speculate tetraradical intermediate **3** formed by spontaneous transannular bond formation in **1b**, similar to the formation of the 1,4-benzene diradical generated by a Bergman reaction.^[30,31] Consequently, in two-dimensionally aligned DBAs, such as **1**, we hypothesize a topochemical polymerization could occur involving *both* butadiyne units in a molecule with transannular bond formation to yield *peri*-benzopolyacene **4** with a fluoranthene substructure. Moreover, the dehydrogenation reaction (Scholl type reaction)^[32] of benzopolyacene **4** might convert it into a more planarized, graphene-like ribbon.^[33] Regarding this connection, we became interested in structural control of 2D molecular networks of DBAs on a surface to investigate their reactivity toward external stimuli. To this end, the supramolecular networks of tetraalkoxy-substituted DBAs **1c–g** at the 1,2,4-trichlorobenzene (TCB) or 1-phenyloctane/

graphite interface were probed systematically using STM. Three different structural motifs (porous, dense linear, and lamella) were observed. We discuss here the factors which determine 2D network structures of DBAs, highlighting the alkyl chain length effect and concentration dependency. Moreover, since we found that in the lamella structure the intermolecular distance between two butadiyne units of DBAs is relatively short compared to those in other structures, their reactivity toward irradiation by an electronic pulse from an STM tip or UV irradiation was investigated.

Results and Discussion

Syntheses of DBAs: Syntheses of DBAs **1c–g** were performed by homocoupling reaction of dialkoxydiethynylbenzenes under Hay conditions.^[13c] Details are described in the Supporting Information.

STM Observation of 2D molecular networks of DBAs at a liquid/solid interface: All STM observations were performed at the TCB or 1-phenyloctane/graphite interface at 20–25 °C. All images were recorded within 3 h after dropping a solution of the DBA. Two different solute concentrations ($\approx 10^{-4}$ M and $\approx 10^{-5}$ M) for each DBA were probed to evaluate the concentration dependent change of the 2D molecular networks. Illustrated in Figure 1 are the three network structures observed and their models optimized by using molecular mechanics simulations (MM3 parameters). Table 1 summarizes the experimental unit cell parameters of the observed structures, as well as the network density ($d_{\text{structure}}$), which was estimated by dividing the number of molecules in a unit cell (Z) by the unit cell area (area).

The porous structure of **1c** was imaged by dropping a TCB or 1-phenyloctane (only at low concentration) solution on the graphite surface (Figure 1a for a phenyloctane solution and Figure S1 in the Supporting Information for a TCB solution). In the STM images, aromatic moieties are often characterized by bright contrast, owing to high tunneling efficiency compared to other parts of the molecules.^[34] Thus, the bright features correspond to the π -conjugated part of **1c** and the lines consisting of the small dots connecting the bright features are ascribed to adsorbed alkyl chains. All alkyl chains of **1c** are adsorbed on the surface, two of them align parallel to one of the three equivalent graphite main axes (the $\langle 1, -2, 1, 0 \rangle$ directions). The porous structure contains rectangular pores, the sizes of which are measured to be 3.0 nm for corner-to-corner and 2.0 nm for edge-to-edge. The pores are most likely occupied by mobile solvent molecules, which were sometimes imaged as brighter contrast (see Figure S2 in the Supporting Information). The unit cell parameters in the two different solvents are the same ($a = 2.8 \pm 0.1$ nm, $b = 2.8 \pm 0.2$ nm, and $\gamma = 82 \pm 1^\circ$ for phenyloctane and $a = 2.8 \pm 0.1$ nm, $b = 2.8 \pm 0.1$ nm, and $\gamma = 82 \pm 1^\circ$ for TCB). The network density (d_{porous}) of this structure is low (0.129 molecules per nm²). A tentative network model is shown in Figure 1b.

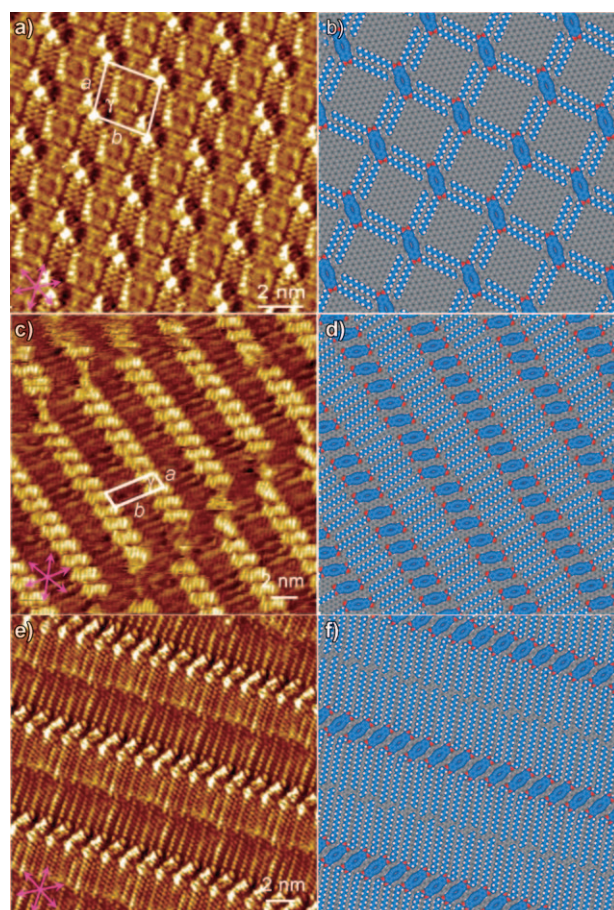


Figure 1. STM images of three types of 2D molecular networks of DBAs and the corresponding network models obtained by molecular mechanics simulations. a) The porous structure of **1c** at the 1-phenyloctane/graphite interface ($I_{\text{sc}} = 0.20$ nA, $V_{\text{bias}} = -0.15$ V, 7.8×10^{-6} M). b) A tentative network model of the porous structure. Periodic boundary condition (5×5 supercell) is $a = 5.563$ nm, $b = 5.546$ nm, and $\gamma = 80.82^\circ$. c) The linear structure of **1d** at the 1-phenyloctane/graphite interface ($I_{\text{sc}} = 0.26$ nA, $V_{\text{bias}} = -0.21$ V, saturated). d) A tentative network model of the linear structure. Periodic boundary condition (3×2 supercell) is $a = 3.076$ nm, $b = 7.040$ nm, and $\gamma = 76.34^\circ$. Two alkyl chains per molecule orienting to the solution phase are omitted for clarity. e) The lamella structure of **1f** at the 1-phenyloctane/graphite interface ($I_{\text{sc}} = 0.26$ nA, $V_{\text{bias}} = -0.21$ V, 2.7×10^{-5} M). f) A tentative network model of the lamella structure. Periodic boundary condition (3×1 supercell) is $a = 3.023$ nm, $b = 6.040$ nm, and $\gamma = 87.15^\circ$. The pink colored arrows in the STM images point the direction of the three equivalent graphite axes (the $\langle 1, -2, 1, 0 \rangle$ directions).

The dense linear structure (Figure 1c) was observed only for a phenyloctane solution of **1d** at a high concentration. In a domain, all π cores of **1d** adopt the same orientation forming a molecular row. The rows were connected through interdigitated alkyl chains. Two alkyl chains per molecule are adsorbed on the surface aligning parallel to one of the graphite axes (the $\langle 1, -2, 1, 0 \rangle$ directions), although the other two chains were not observed on the surface, they are most probably moving freely in the solution phase. A tentative network model of the linear structure is shown in Figure 1d. The unit cell parameters are $a = 1.0 \pm 0.1$ nm, $b =$

Table 1. Structural parameters of monolayers of DBAs **1c–g**.^[a]

Compound	Structure	Concentration [× 10 ⁻⁴ M]	<i>a</i> [nm]	<i>b</i> [nm]	γ [°]	<i>Z</i> ^[b]	<i>m</i> ^[c]	Azimuthal angle θ [°]	Area [nm ²]	Density [molecules per nm ²] ^[d]
1c	porous (TCB)	1.2	2.8±0.1	2.8±0.1	82±1	1	4	36	7.76	0.129 (9.27)
	porous (phenyloctane) ^[e]	0.078	2.8±0.1	2.8±0.2	82±1	1	4	36	7.76	0.129 (9.27)
	lamella (phenyloctane)	0.15–1.0	1.0±0.1	4.3±0.1	83±1	1	4	25	4.27	0.234 (16.9)
1d	lamella (TCB)	0.14–4.1	1.0±0.1	4.8±0.2	85±1	1	4	32	4.78	0.209 (16.7)
	linear (phenyloctane)	saturated	1.0±0.1	3.4±0.2	75±1	1	2	41	3.29	0.305 (15.8)
	lamella (phenyloctane)	0.39	1.0±0.1	4.9±0.2	85±1	1	4	27	4.88	0.205 (16.4)
1e	lamella (TCB)	0.28–2.8	0.94±0.09	5.4±0.1	87±2	1	4	30	5.07	0.197 (17.4)
	lamella (phenyloctane)	0.28–saturated	1.0±0.1	5.4±0.1	87±2	1	4	30	5.39	0.185 (16.3)
	lamella (TCB)	0.25–2.4	1.0±0.2	5.9±0.2	87±1	1	4	29	5.89	0.170 (16.3)
1f	lamella (phenyloctane)	0.27–saturated	1.0±0.1	5.9±0.1	87±1	1	4	30	5.89	0.170 (16.3)
	lamella (TCB)	0.29–2.9	1.1±0.1	6.4±0.2	88±1	1	4	31	7.04	0.142 (14.8)
	lamella (phenyloctane)	0.12–saturated	1.0±0.1	6.4±0.1	87±1	1	4	31	6.39	0.157 (16.3)

[a] For all compounds, the same structures were observed in the different solvents. Structural parameters of networks observed in different solvents are identical within experimental errors. [b] Number of molecules per unit cell. [c] Number of adsorbed alkyl chains per DBA molecule. [d] The value, (number of adsorbed carbon and oxygen atoms)/(area per unit cell), is given in parentheses. [e] The lamella structure was also observed at this concentration (surface coverage, porous/lamella = 7:13).

3.4±0.2 nm, and γ=75±1°. Owing to the dense packing mode, the unit cell area is small and the network density is relatively high (*d*_{linear}=0.305 molecule per nm²).

The lamella structure was observed for **1c** (Figure S3) and **1d** (Figure S4 and S5) under the conditions (i.e., solvents and concentrations) other than those described above. On the other hand, DBAs **1e–g** with longer alkyl chains form only the lamella structure under all conditions examined (Figures S6–S10). A representative STM image and a structural model of the lamella structure are shown in Figures 1e and f, respectively, for **1f** at the phenyloctane/graphite interface. The DBA core of **1f** adopts the same orientation forming a molecular row. All alkyl chains of **1f** align parallel to one of the graphite axes (the <1,−2,1,0> directions) filling the space between the rows of the DBA core. Unlike **1d**, the alkyl chains are not interdigitated, forming a 1D lamella structure. A modeling study reveals two methylene units in two of the alkyl chains most likely adopt an unfavorable eclipsed conformation to achieve favorable intermolecular van der Waals interactions. For the unit cell parameters of the lamella structures of **1c–f**, the vector *a*, which corresponds to intermolecular distance within a row and angle γ are constant (≈1.0 nm and from 83° to 87°), whereas the vector *b* which corresponds to the lamella distance becomes larger upon elongation of the alkyl chains (Table 1).

Notably, we often observed the formation of multilayers of the lamella structures for all compounds.^[35] For instance, in the case of **1f**, each layer was imaged with different con-

trasts, as shown in Figure 2a. At the lower part in Figure 2a, the relatively brighter lines (the blue line is overlaid) correspond to the π cores of **1f** in the upper layer, whereas the fuzzy lines (the red line is overlaid) are those in the lower layer. Average distances between the lines of same contrast are 5.8 nm (upper layer, *l*₁) and 5.9 nm (lower layer, *l*₂). These values are similar to the unit cell vector *b* of the lamella structure of **1f**, indicating that both layers adopt the lamella structure. In addition, though areas are quite small, three different contrasts were observed in an image, indicating the formation of a third layer (the yellow circle in Figure 2b). The observed angles between the bright lines of different layers are mostly 0 or 60° (Figure 2b), but are rarely 90°, suggesting specific interaction between the layers. To estimate the dependence of interlayer interaction on the interlayer angle, we carried out MM3 simulations for an alkane bilayer on graphite, as a model system, by varying the interlayer angle (see the Supporting Information). Interestingly, minimum potentials were located at the angle of 60° (and 120°) and the second minima with nearly equal potentials at 0° (180°) and 90°. These results suggest that the multilayer formation is driven by favorable alkyl–alkyl interactions between layers. A tentative model structure of a bilayer of lamella structure of **1f** with an interlayer angle of 60° is shown in Figure 2c.

Alkyl chain length effect and concentration dependency: It is well known that 2D molecular network structures of

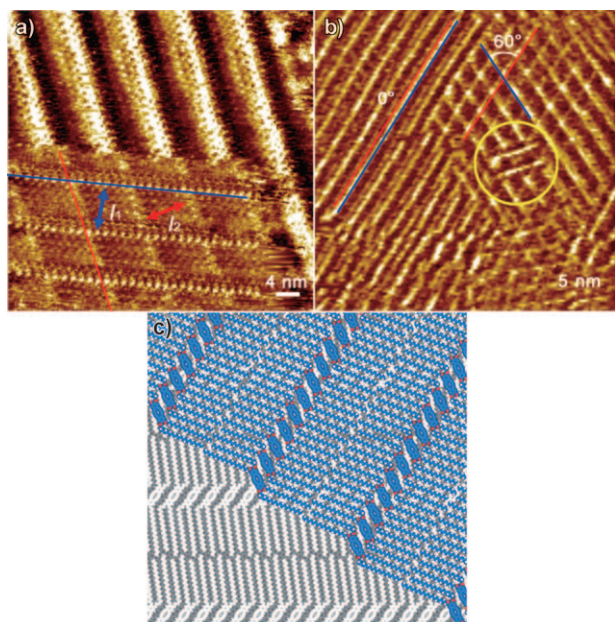


Figure 2. a) An STM image of the double layered lamella structure of **1f** at the TCB/graphite interface ($I_{\text{sc}}=0.22 \text{ nA}$, $V_{\text{bias}}=-0.30 \text{ V}$, $2.5 \times 10^{-4} \text{ M}$). The blue and red lines are overlaid on the upper and lower layers, respectively. Values l_1 and l_2 correspond to the distances between the molecular rows with same contrast. b) An STM image of the multilayered lamella structure of **1g** at the TCB/graphite interface ($I_{\text{sc}}=0.16 \text{ nA}$, $V_{\text{bias}}=-1.69 \text{ V}$, $5.6 \times 10^{-5} \text{ M}$). The yellow circle indicates a triple layer. c) Tentative model of the bilayered lamella structure (interlayer angle is 60°) of **1f** on graphite. The white-colored molecules form the underlying lamella structure.

alkyl-substituted molecules are often affected by the alkyl-chain length because of the shift of balance between intermolecular and molecule–surface van der Waals interactions.^[36] In addition, in some cases, the network structures are concentration-dependent too and thus different structures emerge upon the modulation of solute concentration.^[17] For example, the molecular networks of alkoxy-substituted triangular dehydrobenzo[12]annulene derivatives with short alkyl chains (C_{10} – C_{12}) tend to form porous honeycomb patterns, whereas those with long chains (C_{14} – C_{20}) exhibit dense nonporous linear structures.^[17a] However, the porous honeycomb structures become dominant upon dilution of the solution even in the case of those DBAs with long alkyl chains.

A similar trend was observed in the present system. The structural change is relatively simple if TCB is used as a solvent. DBA **1c**, with the shortest alkyl chain, forms the porous structure, whereas DBAs **1d**–**g** form lamella structures at all concentrations examined. On the other hand, the concentration dependency of network structure was more variable in phenyloctane; the lamella structure of **1c** was observed at higher concentration, whereas the porous structure appears upon dilution. In the case of **1d**, the dense linear structure was observed at high concentration (Figures 1c and d), whereas the lamella structure formed at low concentration. Further elongation of the alkyl chains, however, led

to exclusive formation of the lamella structure at all concentrations investigated. Although the reason for the different solvent effect is difficult to elucidate, the differences in solvation and solvent–substrate interactions most likely play a major role. As for the formation of the porous structure of **1d**, both solvents most likely stabilize this pattern by co-adsorption in the pores (Figure S2).

The dependency of the network structures on alkyl chain and solute concentration can be basically interpreted in term of intermolecular and molecule–substrate interactions per unit area.^[17] The density ($d_{\text{structure}}$) of the three network structures of a DBA with a given alkyl chain length follows the order of porous < lamella ≤ linear (Table 1). To avoid the formation of large void space on the surface, the DBAs with long alkyl chains are prone to form the dense linear and lamella structures because of large intermolecular and molecule–substrate interactions per unit area. The concentration dependency observed for **1c** and **1d**, which have relatively short alkyl chains, in phenyloctane is in accord with this idea. At high concentration the molecules tend to pack more densely, whereas the structure with low molecular density is favored upon dilution, because the difference of intermolecular and molecule–substrate interactions per unit area between the nonporous and porous structures is not so large. In other words, the molecules tend to cover the surface as widely as possible upon dilution.^[17a,f] Moreover, the unique formation of the porous structure of **1c** can be attributed to stabilization, owing to co-adsorption of solvent (vide supra) and/or epitaxial effect (vide infra).^[37]

For **1d**, the unique appearance of the linear structure can be ascribed to epitaxial registry matching between the overlayer and the graphite lattice. Indeed, in the STM images of the linear structure, an apparent Moiré pattern of the alkyl chains along the unit cell vector a was observed (see Figure S11 in the Supporting Information), indicating the existence of long-range ordering (beyond the unit cell).^[38,39] To analyze possible lattice registry, an EpiSearch subroutine of the EpiCalc program was performed.^[40] The program calculates a V/V_0 value, which is a dimensionless potential for each azimuthal angle, showing the degree of commensurism between the overlayer and the substrate layer ($V/V_0=1$ for incommensurism, $V/V_0=0.5$ for point-on-line coincidence, and $V/V_0=0$ for commensurism on nonhexagonal substrate). Perfect commensurism, “point-on-point” coincidence, with graphite lattice was found for the linear structure by assuming a 6×8 supercell ($V/V_0=0.01$, $\theta=40.88^\circ$, $b_1=6.510 \text{ nm}$, $b_2=25.920 \text{ nm}$, $\beta=74.40^\circ$). The Moiré pattern observed experimentally (Figure S11), however, does not fit the above results, it indicates the existence of periodicity by four unit cells each along the unit-cell vector a . To assess the epitaxial effect for the porous structure of **1c** the same analysis was undertaken. As a result, it also revealed perfect commensurism (4×6 supercell, $V/V_0=0.00$, $\theta=36.59^\circ$, $b_1=10.720 \text{ nm}$, $b_2=17.220 \text{ nm}$, $\beta=83.40^\circ$). Conversely, the lamella structures of all DBAs **1c**–**g** did not exhibit perfect commensurism hits even assuming supercells (up to 8×8). These results indicate that the unique formation of the linear structure of

1d and the porous structure of **1c** is attributed, at least partially, to the epitaxial stabilization.

Attempted 2D topochemical polymerization: Topochemical 1,4-polymerization of diacetylenic compounds induced by heat and photoirradiation to produce poly(butadiyne) derivatives in the crystalline state has been well studied.^[41] Design and control of the arrangement of butadiyne units in crystals that utilize weak intermolecular interactions have proven successful to achieve topochemically controlled reactions.^[42] On the basis of the 3D crystal structures of numerous diacetylene monomers and those of the resulting polymers, it was found that maximal reactivity toward polymerization was observed if the distance between two adjacent diacetylene moieties is shorter than 5.0 Å and the tilt angle between the axis of the array and the diacetylene rod is 45°. There are also examples of two-dimensionally confined polymerization of diacetylenic compounds induced by external stimuli. For example, the reaction of diacetylene-containing isophthalic-acid derivative at the liquid/graphite interface upon UV irradiation has been reported by De Schryver, De Feyter et al.^[20a,c] Aono et al. demonstrated polymerization of carboxy-substituted butadiyne derivatives on a graphite surface triggered by irradiation of electronic pulse from an STM tip.^[20b] In some of these reports, the structural parameters of butadiyne units on the graphite surface were also discussed. The intermolecular distances were found to be shorter than 5.0 Å and the tilt angles were approximately 50°, indicating the geometrical requirement for topochemical polymerization on the surfaces is similar to those in 3D crystals.^[20]

As described in the introduction, attempted topochemical polymerization of DBA derivatives in the crystalline state has not been successful.^[27,29] On the other hand, in view of the high reactivity of DBA **1b** toward a transannular reaction,^[26] we envisioned that, in two-dimensionally aligned DBAs, such as **1**, topochemical polymerization would occur involving *both* butadiyne units in a molecule with transannular bond formation to yield *peri*-benzopolyacene **4** (see Scheme 1) with a fluoranthene substructure. A structural subunit of this polymer, rubicene (**5**), has been known for over 100 years (Figure 3a).^[43] The largest known fragment of **4**, to our knowledge, is indenorubicene derivative **6** formed by a domino radical cycloaromatization of an arylalkyne precursor having three butadiyne units.^[44] To assess the feasibility of an even larger structure like polymer **4**, structure optimization of a model compound **7** consisting of five fluoranthene units was undertaken by using DFT methods at the B3LYP/6-31G(d) level of theory (Figure 3b). As shown in Figure 3b, each *peri*-fused indene units winds up and down from the hexacene backbone because of the overcrowding commonly observed in helicenes. Indeed, the dihedral angles of the bonds forming the *fiord* region of **7** range from 14.9 to 22.7° for the inner aromatic rings and 4.9 to 9.0° for the five-membered rings. These torsion angle are smaller than those observed in [6]helicenes (see Figure S15 in the Supporting Information).^[45] The edge-to-edge twist

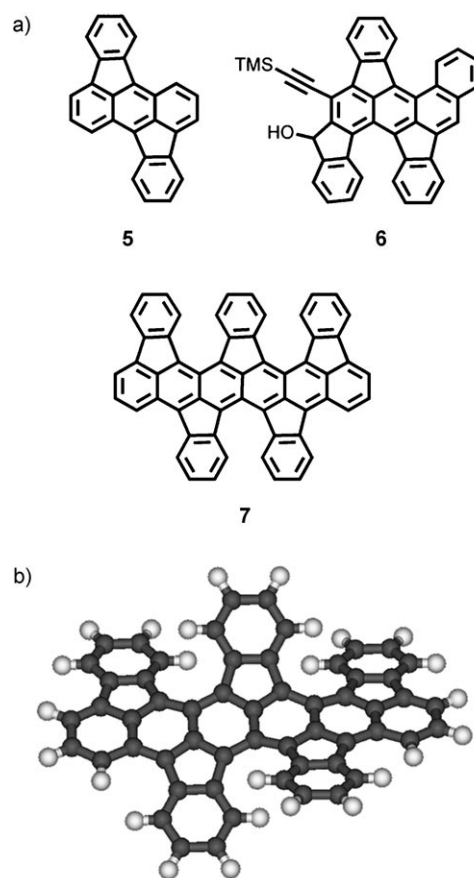


Figure 3. a) Chemical structures of rubicene **5**, a indenorubicene derivative **6**, and a model compound **7** consisting of five fluoranthene units. b) Structure of **7** optimized by B3LYP/6-31G(d) level of theory under C_2 symmetric constraint.

angle of the hexacene backbone of **7** is 49.7°, which is larger than those of benzannelated pentacenes (41–43°),^[46] but is much smaller than those observed for the Pascal's twisted acenes.^[47] These results suggest that *peri*-benzopolyacene **4** is a realistic target at least in terms of structural and thermodynamic aspects. Oligomeric short fragments may well exist.

Molecular modeling of the lamella structures of all DBAs by molecular mechanics simulations reveal that the closest distance between C1 of the butadiyne units of neighboring DBAs should be 5.9–6.1 Å (Figure 4a). For the dense linear structure of **1d**, the corresponding distance is longer (≈6.6 Å, Figure 4b). Clearly the distance between the butadiyne units in the porous structure of **1c** is much longer. Therefore, we investigated possibility of reaction of DBAs in the lamella and linear structures toward external stimuli. We attempted first in-situ irradiation of electronic pulse from an STM tip (2.0–4.0 V) to the lamella structures of **1c** and **1g** at the 1-phenyloctane/graphite interface.^[48] However, we did not observe any change of the monolayer structures of the DBAs (see the Supporting Information). Second, we investigated the effect of UV irradiation to the lamella structures of DBAs **1c**, **1f**, and **1g** and the linear structure of **1d** under air (i.e., by using a dry film obtained by slow

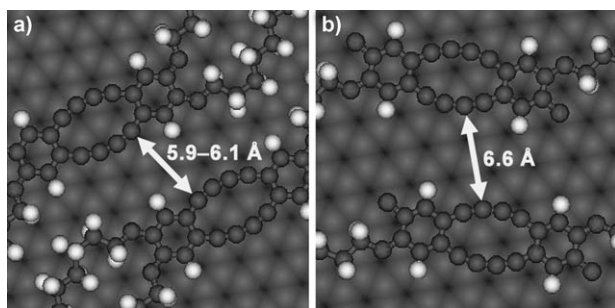


Figure 4. The network models for the a) lamella and the b) linear structures showing the closest intermolecular C–C distance between the diacetylene units.

evaporation of the solvent, see Figure S12 in the Supporting Information), as well as the lamella structure of **1g** at the 1-phenyloctane/graphite interface. Again, no changes of the monolayer structures were observed by subsequent STM investigations (see the Supporting Information). Thus, we were unable to detect any evidence for 2D topochemical oligomerization/polymerization of the DBAs. Plausible reasons for the inertness of the DBAs are unfavorable geometries for the reaction, that is, long diacetylene–diacetylene distance (the distance between C1 and C4 of the butadiyne units of neighboring DBAs in the lamella structure is $\approx 6 \text{ \AA}$), and the large structural change imposed on planar DBAs to transform into nonplanar oligomers.

Conclusion

We have carried out STM investigations on self-assembled monolayers of tetraalkoxy-substituted DBAs **1e–g** at the TCB or phenyloctane/graphite interface. Three types of structures, porous, linear, and lamella structures, were formed and the appearance of which was changed by altering the alkyl chain length, concentration, and the choice of solvent. DBA **1c**, which has the shortest alkyl chain, favors formation of the porous structure in both solvents, whereas for phenyloctane, the dense lamella structure appears at a high solute concentration. DBA **1d** adopts the linear pattern at high solute concentration in phenyloctane, whereas it transforms to the lamella pattern upon dilution. The lamella structure of **1d** was also observed in TCB. The other DBA derivatives **1e–g** form only the dense lamella structure at all conditions examined. The selection in the networks is basically interpreted in terms of intermolecular and molecule–substrate interactions per unit area and network density. The unique appearance of the linear structure of **1d** is attributed to a favorable epitaxial registry matching between the substrate lattice and overlayer lattice. Similarly, the formation of porous structure of **1c** is owed, partly, to the epitaxial effect and solvent co-adsorption. The multilayer formation of the lamella structures was observed and was attributed to favorable interlayer alkyl–alkyl van der Waals interactions.

The reactivity of DBAs in the lamella or linear structures by external stimuli (electronic pulse from an STM tip and UV irradiation) was investigated aiming at 2D topochemical polymerization to afford a novel polymer, *peri*-benzopolyacene **4**. The structural feasibility of **4** was assessed based on the DFT calculations for the model compound **7** having five fluoranthene units. Even though each fluoranthene unit of **7** is highly deformed from planarity, such deformation is not surprising in view of the presence of helicene-like substructures. These results suggest that polymer **4**, at least for its small fragments, is not unrealistic in terms of its structural aspect. However, no evidence for the proposed polymerization was obtained. This is probably owed to unfavorable geometries, that is, long diacetylene–diacetylene distances, and large structural change imposed on planar DBAs to transform into nonplanar oligomers. The present results indicate the necessity for further changes to design a suitable system for the on-surface construction of structurally novel conjugated polymers, which are otherwise difficult to prepare.

Experimental Section

Syntheses of DBAs: Syntheses of DBAs **1e–g** were performed by homo-coupling reaction of dialkoxydiethynylbenzenes under Hay conditions.^[13c] Details are described in the Supporting Information.

STM investigation: All experiments were performed at 20–25 °C by using a Nanoscope IIIa (Digital Instruments Inc.) with an external pulse/function generator (model HP 8111a or Agilent 33220A) with a negative sample bias. The STM image in Figure 1b was acquired in the constant current mode, and the other images were acquired in the variable current mode. Tips were electrochemically etched in a 2 M KOH/6 M KCN solution in water or mechanically cut from Pt/Ir wire (80%/20%, diameter 0.2 mm). Prior to imaging, a compound under investigation was dissolved in commercially available anhydrous 1,2,4-trichlorobenzene (TCB, Aldrich) or 1-phenyloctane (TCI) at two different concentrations ($\approx 10^{-4} \text{ M}$ and 10^{-5} M), and a drop of this solution was applied on a freshly cleaved surface of HOPG (grade ZYB, Momentive Performance Material Quartz Inc., Strongsville, OH). The STM investigations were then performed at the liquid/solid interface. By changing the tunneling parameters during the STM imaging, namely, the voltage applied to the substrate and the average tunneling current, it was possible to switch from the visualization of the adsorbate layer to that of the underlying HOPG substrate. This enabled us to correct for drift effects by the use of SPIP software (Image Metrology A/S). The unit cell parameters were determined from more than 47 experimental data of at least two calibrated STM images.

Molecular mechanics simulations: Molecular mechanics simulations were performed by using the Tinker package and the MM3 force field,^[49] which has been recently reparameterized to take into account weak non-bonding interactions, such as π – π stacking, CH– π interactions, and hydrogen bonds.^[50]

Each starting geometry was built from a molecular model, which was obtained from optimization by the PM3 method under D_{2h} symmetric constraints. Then, the orientation of the π system and alkyl chains was determined from the STM image, and the conformation of some alkyl chains was adjusted by rotating only a minimum number of C–C bonds to fit the experimentally obtained unit cell parameters. The network models were placed at 0.35 nm above the first layer of a periodic two-layer sheet of graphite (interlayer distance of graphite is also 0.35 nm) and adjusted to make the alkyl chains align parallel to the directions of graphite symmetry axes (the $\langle 1, -2, 1, 0 \rangle$ directions). Periodic boundary conditions were employed to fit the experimental unit cell or sometimes the super-

lattice (a few unit cells). The graphite structure was frozen during the simulation, and a cutoff of 2.0 nm was applied from the van der Waals interactions (Lennard-Jones type).

Lattice registry analysis: An epitaxial interface can be described by seven parameters, an overlayer lattice (b_1 , b_2 , and β) and a substrate lattice (a_1 , a_2 , and α), and azimuthal angles (θ), between the lattice vectors a_1 and b_1 . The substrate and overlayer lattice vectors for a given azimuthal orientation θ are related through the transformation matrix [C] in Equation (1) in which the matrix coefficients (p , q , r , and s) are defined by Equations (2)–(5).^[11]

$$\begin{bmatrix} b_1 \\ b_2 \end{bmatrix} = [C] \begin{bmatrix} a_1 \\ a_2 \end{bmatrix} = \begin{bmatrix} p & q \\ r & s \end{bmatrix} \begin{bmatrix} a_1 \\ a_2 \end{bmatrix} \quad (1)$$

$$p = b_1 \sin(\alpha - \theta) / a_1 \sin(\alpha) \quad (2)$$

$$q = b_1 \sin(\theta) / a_2 \sin(\alpha) \quad (3)$$

$$r = b_2 \sin(\alpha - \theta - \beta) / a_1 \sin(\alpha) \quad (4)$$

$$s = b_2 \sin(\theta + \beta) / a_2 \sin(\alpha) \quad (5)$$

The analyses of registry between the molecular layer and substrate layer were performed by using EpiCalc program developed by Ward and co-workers.^[40] EpiCalc determines the lattice registry by rotating an overlayer lattice (b_1 , b_2 , and β) on a substrate lattice (a_1 , a_2 , and α) through a series of azimuthal angles (θ). In the present study, following values were employed as the unit cell parameters of the substrate (graphite; $a_1 = a_2 = 0.246$ nm and $\alpha = 60^\circ$). The program calculates V/V_0 value which is dimensionless potential for each azimuthal angle, showing the degree of commensurism between overlayer and substrate layer ($V/V_0 = 1$ for in-commensurism, $V/V_0 = 0.5$ for point-on-line coincidence, and $V/V_0 = 0$ for commensurism on nonhexagonal substrate). All analyses were performed within the experimental errors of unit cell parameters by increment of 0.01 nm for unit cell vectors and 0.1° for unit cell angle. The variation of azimuthal angle ($\Delta\theta$) was 0.01° . Overlayer size was set to 25×25 . A supercell was assumed up to 8×8 . Threshold value of V/V_0 was set 0.1 to find “point-to-point (POP) coincident” as well as to exclude the numerous “point-on-line (POL) coincident” hits.

DFT calculation: All theoretical calculations were performed with the Gaussian 03 package.^[51] B3LYP calculations with the 6-31G(d) bases sets were used for the geometry optimization of model compound **7**. Compound **7** adapts C_2 symmetric structure at the energy minimum, and the structures without symmetric constraint (C_1 symmetry) has slightly larger energy (1.00 kcal mol⁻¹). The nature of the stationary points was assessed by means of vibration frequency analysis.

Acknowledgements

This work was supported by a Grant-in-Aid for Scientific Research from the Ministry of Education, Culture, Sports, Science, and Technology, Japan, and the US National Science Foundation. C.A.J. acknowledges the NSF-IGERT program for a fellowship and for a travel grant to Japan.

- [1] a) J. Frommer, *Angew. Chem.* **1992**, *104*, 1325–1357; *Angew. Chem. Int. Ed. Engl.* **1992**, *31*, 1298–1328; b) D. M. Walba, F. Stevens, N. A. Clark, D. C. Parks, *Acc. Chem. Res.* **1996**, *29*, 591–597; c) J. V. Barth, *Annu. Rev. Phys. Chem.* **2007**, *58*, 375–407; d) J. A. Theobald, N. S. Oxtoby, M. A. Phillips, N. R. Champness, P. H. Beton, *Nature* **2003**, *424*, 1029–1031; e) L. C. Giancarlo, G. W. Flynn, *Acc. Chem. Res.* **2000**, *33*, 491–501; f) P. Samorí, J. P. Rabe, *J. Phys. Condens. Matter* **2002**, *14*, 9955–9973; g) S. De Feyter, F. C. De Schryver, *J. Phys. Chem. B* **2005**, *109*, 4290–4302; h) J. V. Barth, G. Costantini, K. Kern, *Nature* **2005**, *437*, 671–679; i) L.-J. Wan, *Acc. Chem. Res.* **2006**, *39*, 334–342; j) B. A. Hermann, L. J. Scherer, C. E. Housecroft, E. C. Constable, *Adv. Funct. Mater.* **2006**, *16*, 221–235; k) M.

Surin, P. Samorí, *Small* **2007**, *3*, 190–194; l) K. E. Plass, A. L. Grzesiak, A. J. Matzger, *Acc. Chem. Res.* **2007**, *40*, 287–293; m) J. A. A. W. Elemans, S. Lei, S. De Feyter, *Angew. Chem.* **2009**, *121*, 7434–7469; *Angew. Chem. Int. Ed.* **2009**, *48*, 7298–7332.

- [2] a) C. Joachim, J. K. Gimzewski, A. Aviram, *Nature* **2000**, *408*, 541–548; b) A. Nitzan, M. A. Ratner, *Science* **2003**, *300*, 1384–1389.
- [3] J. R. Sheats, B. W. Smith, *Microlithographic Science and Technology*, 1st ed., Marcel Dekker, New York, **1999**.
- [4] a) G. M. J. Schmidt, *Pure Appl. Chem.* **1971**, *27*, 647–678; b) *Crystal Engineering: The Design of Organic Solid* (Ed.: G. R. Desiraju), Elsevier, Amsterdam, **1989**; c) G. R. Desiraju, *Angew. Chem.* **1995**, *107*, 2541–2558; *Angew. Chem. Int. Ed. Engl.* **1995**, *34*, 2311–2327; d) N. Blagden, R. J. Davey, *Cryst. Growth Des.* **2003**, *3*, 873–885.
- [5] S. Furukawa, S. De Feyter, *Top. Curr. Chem.* **2009**, *287*, 87–133.
- [6] There are a number of reports about the formation of 2D molecular networks through hydrogen bonding as connectivity. See, for example: a) S. Griessl, M. Lackinger, M. Edelwirth, M. Hietschold, W. M. Heckl, *Single Mol.* **2002**, *3*, 25–31; b) S. J. H. Griessl, M. Lackinger, F. Jamitzky, T. Markert, M. Hietschold, W. M. Heckl, *Langmuir* **2004**, *20*, 9403–9407; c) S. B. Lei, C. Wang, S. X. Yin, H. N. Wang, F. Xi, H. W. Liu, B. Xu, L. J. Wan, C. L. Bai, *J. Phys. Chem. B* **2001**, *105*, 10838–10841; d) J. Otsuki, E. Nagamine, T. Kondo, K. Iwasaki, M. Asakawa, K. Miyake, *J. Am. Chem. Soc.* **2005**, *127*, 10400–10405; e) W. Mamdouh, R. E. A. Kelly, M. Dong, L. N. Kantorovich, F. Besenbacher, *J. Am. Chem. Soc.* **2008**, *130*, 695–702.
- [7] a) T. Yokoyama, S. Yokoyama, T. Kamikado, Y. Okuno, S. Mashiko, *Nature* **2001**, *413*, 619–621; b) M. de Wild, S. Berner, H. Suzuki, H. Yanagi, D. Schlettwein, S. Ivan, A. Baratoff, H.-J. Guentherodt, T. A. Jung, *ChemPhysChem* **2002**, *3*, 881–885; c) Y. Wei, W. Tong, C. Wise, X. Wei, K. Armbrust, M. Zimmt, *J. Am. Chem. Soc.* **2006**, *128*, 13362–13363; d) Y. Wei, W. Tong, M. B. Zimmt, *J. Am. Chem. Soc.* **2008**, *130*, 3399–3405.
- [8] a) M. A. Lingenfelder, H. Spillmann, A. Dmitriev, S. Stepanow, N. Lin, J. V. Barth, K. Kern, *Chem. Eur. J.* **2004**, *10*, 1913–1919; b) S. Stepanow, N. Lin, D. Payer, U. Schilckum, F. Klappenberg, G. Zoppellaro, M. Ruben, H. Brune, J. V. Barth, K. Kern, *Angew. Chem.* **2007**, *119*, 724–727; *Angew. Chem. Int. Ed.* **2007**, *46*, 710–713; c) M. Surin, P. Samorí, A. Jouaiti, N. Kyritsakas, M. W. Hosseini, *Angew. Chem.* **2007**, *119*, 249–253; *Angew. Chem. Int. Ed.* **2007**, *46*, 245–249.
- [9] a) X. Qiu, C. Wang, Q. Zeng, B. Xu, S. Yin, H. Wang, S. Xu, C. Bai, *J. Am. Chem. Soc.* **2000**, *122*, 5550–5556; b) D. Bléger, D. Kreher, F. Mathevet, A.-J. Attias, G. Schull, A. Huard, L. Douillard, C. Fiorini-Debuschert, F. Charra, *Angew. Chem.* **2007**, *119*, 7548–7551; *Angew. Chem. Int. Ed.* **2007**, *46*, 7404–7407; c) D. Bléger, D. Kreher, F. Mathevet, A.-J. Attias, I. Arfaoui, G. Metgé, L. Douillard, C. Fiorini-Debuschert, F. Charra, *Angew. Chem.* **2008**, *120*, 8540–8543; *Angew. Chem. Int. Ed.* **2008**, *47*, 8412–8415.
- [10] a) S. Furukawa, H. Uji-i, K. Tahara, T. Ichikawa, M. Sonoda, F. C. De Schryver, Y. Tobe, S. De Feyter, *J. Am. Chem. Soc.* **2006**, *128*, 3502–3503; b) K. Tahara, S. Furukawa, H. Uji-i, T. Uchino, T. Ichikawa, J. Zhang, W. Mamdouh, M. Sonoda, F. C. De Schryver, S. De Feyter, Y. Tobe, *J. Am. Chem. Soc.* **2006**, *128*, 16613–16625.
- [11] a) A. C. Hillier, M. D. Ward, *Phys. Rev. B* **1996**, *54*, 14037–14051; b) D. E. Hooks, T. Fritz, M. D. Ward, *Adv. Mater.* **2001**, *13*, 227–241.
- [12] Y. Yang, C. Wang, *Curr. Opin. Colloid Interface Sci.* **2009**, *14*, 135–147.
- [13] a) W. Mamdouh, H. Uji-i, J. S. Ladislaw, A. E. Dulcey, V. Percec, F. C. De Schryver, S. De Feyter, *J. Am. Chem. Soc.* **2006**, *128*, 317–325; b) K. G. Nath, O. Ivashenko, J. A. Miwa, H. Dang, J. D. Wuest, A. Nanci, D. F. Perepichka, F. Rosei, *J. Am. Chem. Soc.* **2006**, *128*, 4212–4213; c) K. Tahara, C. A. Johnson II, T. Fujita, M. Sonoda, F. C. De Schryver, S. De Feyter, M. M. Haley, Y. Tobe, *Langmuir* **2007**, *23*, 10190–10197.
- [14] a) B. Venkataraman, J. J. Breen, G. W. Flynn, *J. Phys. Chem.* **1995**, *99*, 6608–6619; b) C.-J. Li, Q.-D. Zeng, C. Wang, L.-J. Wan, S.-L. Xu, C.-R. Wang, C.-L. Bai, *J. Phys. Chem. B* **2003**, *107*, 747–750; c) M. Lackinger, S. Griessl, W. M. Heckl, M. Hietschold, G. W. Flynn, *Langmuir* **2005**, *21*, 4984–4988; d) L. Kampschulte, M. Lack-

- inger, A.-K. Maier, R. S. K. Kishore, S. Griessl, M. Schmittel, W. M. Heckl, *J. Phys. Chem. B* **2006**, *110*, 10829–10836; e) X. Shao, X. Luo, X. Hu, K. Wu, *J. Phys. Chem. B* **2006**, *110*, 1288–1293; f) R. Gutzler, S. Lappe, K. Mahata, M. Schmittel, W. M. Heckl, M. Lackinger, *Chem. Commun.* **2009**, 680–682.
- [15] a) A. Stabel, R. Heinz, F. C. De Schryver, J. P. Rabe, *J. Phys. Chem.* **1995**, *99*, 505–507; b) L. Piot, A. Marchenko, J. Wu, K. Müllen, D. Fichou, *J. Am. Chem. Soc.* **2005**, *127*, 16245–16250; c) G. M. Florio, J. E. Klare, M. O. Pasamba, T. L. Werblowsky, M. Hyers, B. J. Berne, M. S. Hybertsen, C. Nuckolls, G. W. Flynn, *Langmuir* **2006**, *22*, 10003–10008.
- [16] a) D. Rohde, C.-J. Yan, H.-J. Yan, L.-J. Wan, *Angew. Chem.* **2006**, *118*, 4100–4104; *Angew. Chem. Int. Ed.* **2006**, *45*, 3996–4000; b) C.-J. Li, Q.-D. Zeng, Y.-H. Liu, L.-J. Wan, C. Wang, C.-R. Wang, C.-L. Bai, *ChemPhysChem* **2003**, *4*, 857–859; c) R. T. Baker, J. D. Mougous, A. Brackley, D. L. Patrick, *Langmuir* **1999**, *15*, 4884–4891.
- [17] a) S. Lei, K. Tahara, F. C. De Schryver, M. Van der Auweraer, Y. Tobe, S. De Feyter, *Angew. Chem.* **2008**, *120*, 3006–3010; *Angew. Chem. Int. Ed.* **2008**, *47*, 2964–2968; b) L. Kampschulte, T. L. Werblowsky, R. S. K. Kishore, M. Schmittel, W. M. Heckl, M. Lackinger, *J. Am. Chem. Soc.* **2008**, *130*, 8502–8507; c) C.-A. Palma, M. Bonini, A. Llanes-Pallas, T. Breiner, M. Prato, D. Bonifazi, P. Samorí, *Chem. Commun.* **2008**, 5289–5291; d) C.-A. Palma, J. Bjork, M. Bonini, M. S. Dyer, A. Llanes-Pallas, D. Bonifazi, M. Persson, P. Samorí, *J. Am. Chem. Soc.* **2009**, *131*, 13062–13071; e) C.-A. Palma, M. Bonini, T. Breiner, P. Samorí, *Adv. Mater.* **2009**, *21*, 1383–1386; f) K. Tahara, S. Okuhata, J. Adisojoso, S. Lei, T. Fujita, S. De Feyter, Y. Tobe, *J. Am. Chem. Soc.* **2009**, *131*, 17583–17590.
- [18] J. Sakamoto, J. van Heijst, O. Lukin, A. D. Schlüter, *Angew. Chem.* **2009**, *121*, 1048–1089; *Angew. Chem. Int. Ed.* **2009**, *48*, 1030–1069.
- [19] a) H. Ozaki, T. Funaki, Y. Mazaki, S. Masuda, Y. Harada, *J. Am. Chem. Soc.* **1995**, *117*, 5596–5597; b) O. Endo, H. Ootsubo, N. Toda, M. Suhara, H. Ozaki, Y. Mazaki, *J. Am. Chem. Soc.* **2004**, *126*, 9894–9895.
- [20] a) P. C. M. Grim, S. De Feyter, A. Gesquière, P. Vanoppen, M. Rücker, S. Valiyaveettil, G. Moessner, K. Müllen, F. C. De Schryver, *Angew. Chem.* **1997**, *109*, 2713–2715; *Angew. Chem. Int. Ed. Engl.* **1997**, *36*, 2601–2603; b) Y. Okawa, M. Aono, *Nature* **2001**, *409*, 683–684; c) Y. Okawa, M. Aono, *J. Chem. Phys.* **2001**, *115*, 2317–2322; d) Y.-H. Qiao, Q.-D. Zeng, Z.-Y. Tan, S.-D. Xu, D. Wang, C. Wang, L.-J. Wan, C.-L. Bai, *J. Vac. Sci. Technol. B* **2002**, *20*, 2466–2469; e) A. Miura, S. De Feyter, M. M. S. Abdel-Mottaleb, A. Gesquière, P. C. M. Grim, G. Moessner, M. Sieffert, M. Klapper, K. Müllen, F. C. De Schryver, *Langmuir* **2003**, *19*, 6474–6482; f) S. Nishio, D. I.-i. H. Matsuda, M. Yoshidome, H. Uji-i, H. Fukumura, *Jpn. J. Appl. Phys.* **2005**, *44*, 5417–5420.
- [21] L. Lafferentz, F. Ample, H. Yu, S. Hecht, C. Joachim, L. Grill, *Science* **2009**, *323*, 1193–1197.
- [22] a) S. Weigelt, C. Busse, C. Bombis, M. M. Knudsen, K. V. Gothelf, E. Laegsgaard, F. Besenbacher, T. R. Linderoth, *Angew. Chem.* **2008**, *120*, 4478–4482; *Angew. Chem. Int. Ed.* **2008**, *47*, 4406–4410; b) M. Treier, N. V. Richardson, R. Fasel, *J. Am. Chem. Soc.* **2008**, *130*, 14054–14055.
- [23] N. A. A. Zwaneveld, R. Pawlak, M. Abel, D. Catalin, D. Gigmes, D. Bertin, L. Porte, *J. Am. Chem. Soc.* **2008**, *130*, 6678–6679.
- [24] a) L. Grill, M. Dyer, L. Lafferentz, M. Persson, M. V. Peters, S. Hecht, *Nat. Nanotechnol.* **2007**, *2*, 687–691; b) M. Bieri, M. Treier, J. Cai, K. Aït-Mansour, P. Ruffieux, O. Gröning, P. Gröning, M. Kastler, R. Rieger, X. Feng, K. Müllen, R. Fasel, *Chem. Commun.* **2009**, 6919–6921.
- [25] a) O. M. Behr, G. Eglinton, R. A. Raphael, *Chem. Ind.* **1959**, 699–700. For a recent review on dehydrobenzoannulenes, see: b) E. L. Spitler, C. A. Johnson II, M. M. Haley, *Chem. Rev.* **2006**, *106*, 5344–5386.
- [26] Q. Zhou, P. J. Carroll, T. M. Swager, *J. Org. Chem.* **1994**, *59*, 1294–1301.
- [27] T. Nishinaga, N. Nodera, Y. Miyata, K. Komatsu, *J. Org. Chem.* **2002**, *67*, 6091–6096.
- [28] I. Hisaki, H. Shigemitsu, Y. Sakamoto, Y. Hasegawa, Y. Okajima, K. Nakano, N. Tohnai, M. Miyata, *Angew. Chem.* **2009**, *121*, 5573–5577; *Angew. Chem. Int. Ed.* **2009**, *48*, 5465–5469.
- [29] In the case of octadehydrotribenzo[14]annulene, however, topochemical polymerization did take place, which is due to the suitable packing for polymerization in crystals. K. P. Baldwin, A. J. Matzger, D. A. Scheiman, C. A. Tessier, K. P. C. Vollhardt, W. J. Youngs, *Synlett* **1995**, 1215–1218.
- [30] For Bergman reactions, see: a) R. R. Jones, R. G. Bergman, *J. Am. Chem. Soc.* **1972**, *94*, 660–661; b) R. G. Bergman, *Acc. Chem. Res.* **1973**, *6*, 25–31; c) T. P. Lockhart, P. B. Comita, R. G. Bergman, *J. Am. Chem. Soc.* **1981**, *103*, 4082–4090.
- [31] The tetraradical intermediate **3** apparently seems much less favorable than 1,4-benzene diradical. However, a very rough estimate of bond dissociation energies indicates that the conversion of DBA **1b** into tetraradical **3** would be endoergic by about 5–6 kcal mol⁻¹. Namely, the bond dissociation energy (56.6 kcal mol⁻¹) of one of π bonds of a triple bond is estimated from the difference between those of ethyne (230.7 kcal mol⁻¹) and ethene (174.1 kcal mol⁻¹). (Four time of this energy) minus (twice of the dissociation energy (116 kcal mol⁻¹) of a vinyl-vinyl bond) yields 5.6 kcal mol⁻¹. The thermochemical data are taken from the following review: S. J. Blanksby, G. B. Ellison, *Acc. Chem. Res.* **2003**, *36*, 255–263.
- [32] a) R. Scholl, J. Mansfeld, *Ber. Dtsch. Chem. Ges.* **1910**, *43*, 1734–1746; b) M. Müller, C. Kübel, K. Müllen, *Chem. Eur. J.* **1998**, *4*, 2099–2109; c) P. Rempala, J. Kroulik, B. T. King, *J. Am. Chem. Soc.* **2004**, *126*, 15002–15003.
- [33] a) J. Wu, L. Gherghel, M. D. Watson, J. Li, Z. Wang, C. D. Simpson, U. Kolb, K. Müllen, *Macromolecules* **2003**, *36*, 7082–7089; b) X. Yang, X. Dou, A. Rouhanipour, L. Zhi, H. J. Räder, K. Müllen, *J. Am. Chem. Soc.* **2008**, *130*, 4216–4217.
- [34] R. Lazzaroni, A. Calderone, G. Lambin, J. P. Rabe, J. L. Brédas, *Synth. Met.* **1991**, *41*, 525–528.
- [35] There are a number of reports about the formation of multilayer. See, for example: a) F. Jäckel, M. Ai, J. Wu, K. Müllen, J. P. Rabe, *J. Am. Chem. Soc.* **2005**, *127*, 14580–14581; b) S. Lei, J. Puigmarti-Luis, A. Minoia, M. Van der Auweraer, C. Rovira, R. Lazzaroni, D. B. Amabilino, S. De Feyter, *Chem. Commun.* **2008**, 703–705; c) D. Takajo, E. Fujiwara, S. Irie, T. Nemoto, S. Isoda, H. Ozaki, N. Toda, S. Tomii, T. Magara, Y. Mazaki, G. Yamamoto, *J. Cryst. Growth* **2002**, 237–239, 2071–2075.
- [36] a) P. Wu, Q. Zeng, S. Xu, C. Wang, S. Yin, C. L. Bai, *ChemPhysChem* **2001**, *2*, 750–754; b) F. Charra, J. Cousty, *Phys. Rev. Lett.* **1998**, *80*, 1682–1685; c) L. Askadskaya, C. Boeffel, J. P. Rabe, *Ber. Bunsen-Ges.* **1993**, *97*, 517–521; d) S. Ito, M. Wehmeier, J. D. Brand, C. Kübel, R. Epsch, J. P. Rabe, K. Müllen, *Chem. Eur. J.* **2000**, *6*, 4327–4342; e) E. Mena-Osteritz, *Adv. Mater.* **2002**, *14*, 609–616.
- [37] The size of each domain in the monolayer of DBAs also depends on a solute concentration. At higher concentration, DBAs tend to form many small domains, whereas the size of domain increases upon dilution. For example, the average domain size of the lamella structure formed by dropping a phenyloctane solution of **1e** at a concentration of 2.8×10^{-4} M is about 1900 nm² (calculated from six large area images (200 × 200 nm)), whereas upon dilution the size of domain becomes over typical scanning size (150 × 150 nm, 22500 nm²).
- [38] The Moiré pattern of monolayers of alkane or alkylated molecules were often observed. See, for example: a) K. E. Plass, K. Kim, A. J. Matzger, *J. Am. Chem. Soc.* **2004**, *126*, 9042–9053; b) S.-B. Lei, C. Wang, X.-L. Fan, L.-J. Wan, C.-L. Bai, *Langmuir* **2003**, *19*, 9759–9763; c) K. E. Plass, A. J. Matzger, *Chem. Commun.* **2006**, 3486–3488; d) A. Stabel, R. Heinz, J. P. Rabe, G. Wegner, F. C. De Schryver, D. Corens, W. Dehaen, C. Süling, *J. Phys. Chem.* **1995**, *99*, 8690–8697; e) S. De Feyter, A. Gesquière, P. C. M. Grim, F. C. De Schryver, S. Valiyaveettil, C. Meiners, M. Sieffert, K. Müllen, *Langmuir* **1999**, *15*, 2817–2822; f) D. M. Cyr, B. Venkataraman, G. W. Flynn, *Chem. Mater.* **1996**, *8*, 1600–1615.
- [39] B. Ilan, G. M. Florio, M. S. Hybertsen, B. J. Berne, G. W. Flynn, *Nano Lett.* **2008**, *8*, 3160–3165.

- [40] EpiCalc was downloaded on the Ward's group web site (<http://www.nyu.edu/fas/dept/chemistry/wardgroup/Software.html>).
- [41] a) G. A. Wagner, *Z. Naturforsch. B* **1969**, *24*, 824–832; b) R. H. Baughman, *J. Polym. Sci. Polym. Phys. Ed.* **1974**, *12*, 1511–1535. For a review, see: c) V. Enkelmann, *Adv. Polym. Sci.* **1984**, *63*, 91–136.
- [42] a) J. J. Kane, R.-F. Liao, J. W. Lauher, F. W. Fowler, *J. Am. Chem. Soc.* **1995**, *117*, 12003–12004; b) Z. Li, F. W. Fowler, J. W. Lauher, *J. Am. Chem. Soc.* **2009**, *131*, 634–643; c) A. Sun, J. W. Lauher, N. S. Goroff, *Science* **2006**, *312*, 1030–1034. For reviews, see: d) F. W. Fowler, J. W. Lauher, *J. Phys. Org. Chem.* **2000**, *13*, 850–857; e) J. W. Lauher, F. W. Fowler, N. S. Goroff, *Acc. Chem. Res.* **2008**, *41*, 1215–1229.
- [43] a) R. Fittig, A. Schltz, *Justus Liebigs Ann. Chem.* **1873**, *166*, 361–382; b) W. Schlenk, M. Karplus, *Chem. Ber.* **1928**, *61*, 1675–1680; c) R. Scholl, H. K. Meyer, *Chem. Ber.* **1932**, *65*, 926–927; d) V. Sachweh, H. Langhals, *Chem. Ber.* **1990**, *123*, 1981–1987; e) M. Smet, R. Shukla, L. Fülpöp, W. Dehaen, *Eur. J. Org. Chem.* **1998**, 2769–2773.
- [44] K. Miyawaki, T. Kawano, I. Ueda, *Tetrahedron Lett.* **2000**, *41*, 1447–1451.
- [45] The dihedral angles of the central aromatic bonds of [6]helicene derivatives range from 26 to 30° and those next to the central bonds range from 12 to 18°; a) D. A. Lightner, D. T. Hefelfinger, T. W. Powers, G. W. Frank, K. N. Trueblood, *J. Am. Chem. Soc.* **1972**, *94*, 3492–3497; b) C. de Rango, G. Tsoucaris, J. P. Delerq, G. Germain, J. P. Putzeys, *Cryst. Struct. Comm.* **1973**, *2*, 189–192; c) G. W. Frank, D. T. Hefelfinger, D. A. Lightner, *Acta Crystallogr. Sect. B* **1973**, *29*, 223–230; d) F. Aloui, R. E. Abed, A. Marinetti, B. B. Hassine, *Tetrahedron Lett.* **2007**, *48*, 2017–2020.
- [46] a) M. G. Rossmann, *J. Chem. Soc.* **1959**, 2607–2613; b) A. Izuoka, K. Wakui, T. Fukuda, N. Sato, T. Sugawara, *Acta Crystallogr. Sect. C* **1992**, *48*, 900–902; c) J. M. Robertson, J. Trotter, *J. Chem. Soc.* **1959**, 2614–2623.
- [47] The largest known end-to-end twist angle of a pentacene unit is 144°; a) J. Lu, D. M. Ho, N. J. Vogelaar, C. M. Kraml, R. A. Pascal, Jr., *J. Am. Chem. Soc.* **2004**, *126*, 11168–11169. For an excellent review on twisted acenes, see: b) R. A. Pascal, Jr., *Chem. Rev.* **2006**, *106*, 4809–4819.
- [48] To confirm reliability of our experimental conditions, we performed control experiments by using a monolayer of 10,12-nonacosadiynoic acid at 1-phenyloctane/graphite interface, which is reported to polymerize on a surface upon application of electronic pulse.^[20f] By applying electronic pulse from an STM tip, the polymerization was indeed observed, indicating validity of our experimental conditions. See also the Supporting Information.
- [49] a) N. L. Allinger, Y. H. Yuh, J. H. Lii, *J. Am. Chem. Soc.* **1989**, *111*, 8551–8566; b) J. H. Lii, N. L. Allinger, *J. Am. Chem. Soc.* **1989**, *111*, 8566–8575; c) J. H. Lii, N. L. Allinger, *J. Am. Chem. Soc.* **1989**, *111*, 8576–8582.
- [50] B. Ma, J. H. Lii, N. L. Allinger, *J. Comput. Chem.* **2000**, *21*, 813–825.
- [51] Gaussian 03, Revision D.01, M. J. Frisch, G. W. Trucks, H. B. Schlegel, G. E. Scuseria, M. A. Robb, J. R. Cheeseman, J. A. Montgomery, Jr., T. Vreven, K. N. Kudin, J. C. Burant, J. M. Millam, S. S. Iyengar, J. Tomasi, V. Barone, B. Mennucci, M. Cossi, G. Scalmani, N. Rega, G. A. Petersson, H. Nakatsuji, M. Hada, M. Ehara, K. Toyota, R. Fukuda, J. Hasegawa, M. Ishida, T. Nakajima, Y. Honda, O. Kitao, H. Nakai, M. Klene, X. Li, J. E. Knox, H. P. Hratchian, J. B. Cross, C. Adamo, J. Jaramillo, R. Gomperts, R. E. Stratmann, O. Yazyev, A. J. Austin, R. Cammi, C. Pomelli, J. W. Ochterski, P. Y. Ayala, K. Morokuma, G. A. Voth, P. Salvador, J. J. Dannenberg, V. G. Zakrzewski, S. Dapprich, A. D. Daniels, M. C. Strain, O. Farkas, D. K. Malick, A. D. Rabuck, K. Raghavachari, J. B. Foresman, J. V. Ortiz, Q. Cui, A. G. Baboul, S. Clifford, J. Ciosowski, B. B. Stefanov, G. Liu, A. Liashenko, P. Piskorz, I. Komaromi, R. L. Martin, D. J. Fox, T. Keith, M. A. Al-Laham, C. Y. Peng, A. Nanayakkara, M. Challacombe, P. M. W. Gill, B. Johnson, W. Chen, M. W. Wong, C. Gonzalez, J. A. Pople, Gaussian, Inc., Wallingford CT, **2005**.

Received: March 21, 2010

Published online: June 30, 2010